Laser-induced surface phonons and their excitation of nanostructures

Markus Schmotz,[1,*] Dominik Gollmer,[1] Florian Habel,[1] Stephen Riedel,[1] and Paul Leiderer[1]

[1] *Department of Physics, University of Konstanz, 78457 Konstanz, Germany*

(Received April 9, 2010)

We report on the generation of surface phonons up to the GHz range utilizing laser interference techniques and analysis based on knife-edge and diffraction methods. Appropriate structure design also gives a route towards more complex SAW optics. Further, we are developing a new detection method based on scanning probe microscopy.

PACS numbers: 43.35.Pt, 68.37.Ef, 42.25.Hz

I. INTRODUCTION

Information about deformations of nanostructures in the gigahertz regime is rather sparse until now. Especially deformations after irradiation with short laser pulses have been studied only recently; see [1] and according references therein. Our work aims at creating surface phonons or surface acoustic waves (SAW) [2] in the gigahertz (GHz) range based on short laser pulse techniques and to employ them to excite nanostructures monochromatically [3]. In the first part, we present experiments, where both generation and detection of SAWs up to the GHz regime are purely optical based. They lead to an investigation of values like travelling speed, damping coefficients or attenuation for the used sample types and we compare these values to literature. The second part shows the development of the Scanning Tunnelling Microscope (STM). Starting with standard lithium-niobate transducer substrates for proof-of-principle, we show the very first results of laser-excited SAWs that are detected via STM.

II. OPTICAL EXPERIMENTS

The generation of SAWs in our approach so far is mostly based on laser interference [4, 5]. For this purpose, a metal film is thermally evaporated onto glass. A grating is then statically burned into the substrates by interference of two coherent laser pulses (seeded Nd:YAG, spot diameter = 5 mm, FWHM = 10 ns, energies ∼100 mJ/pulse) and thus forms an absorption contrast between the metal stripes and the underlying substrate. The grating periods ranged from 8 to 225 μm. By irradiating these structures with a Ti:Sa laser pulse (spot diameter = 5 mm, FWHM = 150 fs, energy = 2 mJ/pulse), SAWs are generated on the basis of the thermal expansion of the metal. As this technique is limited to structure sizes of half of the interfering laser wavelength, another way of generation has

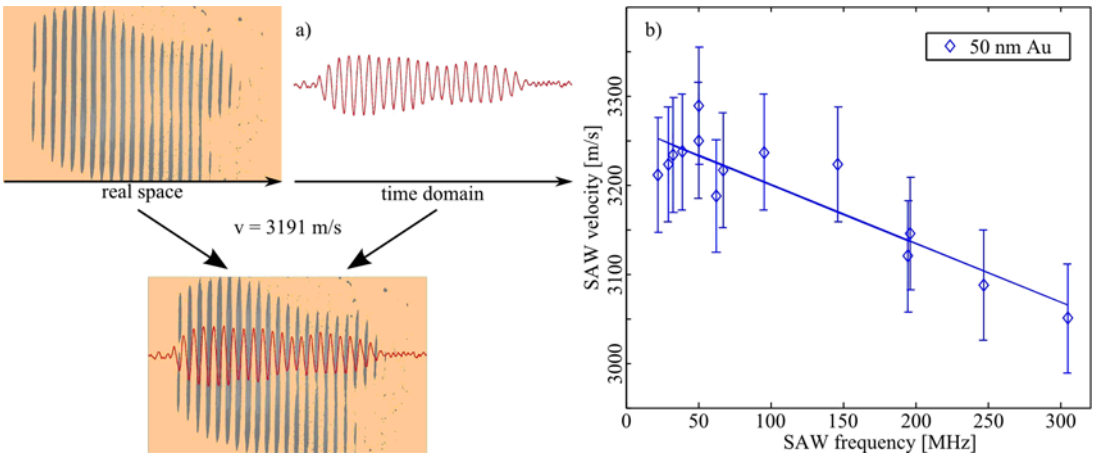

FIG. 1: (a) Micrograph of a permanent grating burned into an Au film by laser interference. The red curve shows the corresponding knife-edge signal at a given distance. Real space and time domain were converted into each other via the Rayleigh velocity of v = 3191 m/s and overlaid manually. Each maximum and minimum can be associated with an Au stripe or the underlying substrate, respectively. (b) With increasing SAW frequency, the Rayleigh velocity shifts due to dispersion as expected.

to be exploited. Using near-field effects underneath colloidal particles [6] or at the edges of nanostructures [7] seems to be a promising candidate, which we are investigating at the moment.

The detection of the SAWs is carried out via knife-edge and diffraction methods [8, 9]. For the knife-edge method, a well focused beam at a certain distance from the grating structure is spatially split into two halves. Each one is then detected with a standard photodiode. The difference between both the detectors is therefore proportional to the local slope of the travelling wave. Comparison of a micrograph of the grating statically burned into the metal film and the corresponding knife-edge signal is shown in Fig.1(a). Every feature of the grating is also visible in the optical measurement. For the case of Au on glass, the absorption and thus thermal expansion of the metal is responsible for the launch of a SAW since glass is transparent at the excitation wavelength. This is confirmed by the exact match of signal maxima to metal stripes. The time domain signals of the knife-edge were transformed into real space using the measured Rayleigh velocity of $v = 3191 m/s$. Both images were then overlaid manually to clarify the effect. Fig.1(b) shows the dispersion relation for Au on glass for the measurable frequency regime up to approximately 300 MHz. The propagation velocity v decreases with increasing frequency because with decreasing wavelength the SAW, is more and more localized in the Au film, where the Rayleigh velocity is typically low. Extrapolation to 0 MHz gives $v = 3266 \pm 30 m/s$ for the pure glass, which fits well to calculated values from literature [10].

For the diffraction method, a laser spot is placed at a given distance from the interference structure. While the wave is travelling beneath, it forms a transient grating which can be detected in the first order of diffraction and only while the SAW is within the

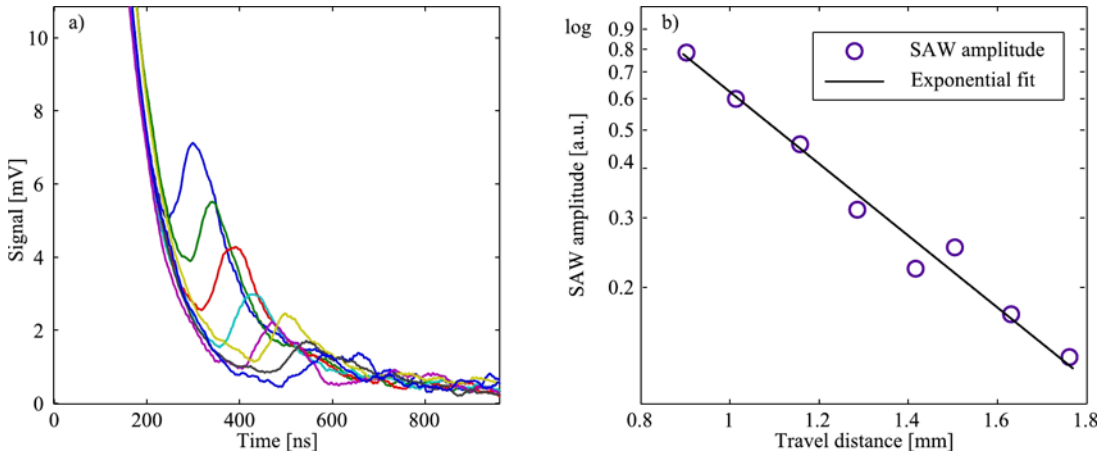

FIG. 2: (a) Diffraction signals of 440-MHz SAWs on Au on glass substrates at different distances from the generation spot. Not only the signal onset is delayed but also the signal height decreases due to damping effects. (b) Detail of the SAW amplitude for increasing travel lengths. The solid line gives an exponential fit to the data, verifying the predicted exponential decay.

probing laser spot. A typical measurement is shown in Fig.2(a), where the steep increase on the left hand side is due to cross-talk of the excitation laser. The subsequent peak is the diffraction signal of the passing SAW. With increasing distance between excitation and probing spot, not only the time delay increases—which can be understood by means of propagation velocity—but also the signal height decreases, see Fig.2(b). The amplitude of the diffraction signal, which is denoted as SAW-amplitude here, follows the expected exponential decay. In this case, with a glass substrate, the damping is 85 dB/cm, which leads to a rather short travelling distance of only 2 mm.

By appropriate shapes of the grating structures SAWs can be focused, see the sketch in Fig.3(a). Here again we use the knife-edge technique described above. We observe an amplitude increase within the focus as much as tenfold compared to the original amplitude. In Fig.3(b), a Gaussian profile is fitted to the focus cross section, verifying that it is formed by superposition of the SAW wave fronts. This demonstrates a route towards more complex SAW optics.

III. SCANNING TUNNELING MICROSCOPE

An approach that should allow one to detect short-wavelength SAWs in the higher GHz regime is to use scanning-probe techniques [11–13]. Therefore, we are developing a detection method based on a homebuilt, variable temperature Scanning Tunnelling Microscope (STM), exploiting the highly nonlinear I(z)-characteristic of the tunnelling gap.

For calibration purposes of the STM signals, we used standard IDT-based (interdigital transducer) SAW devices like $LiNbO_3$. At a distance of some mm away from the

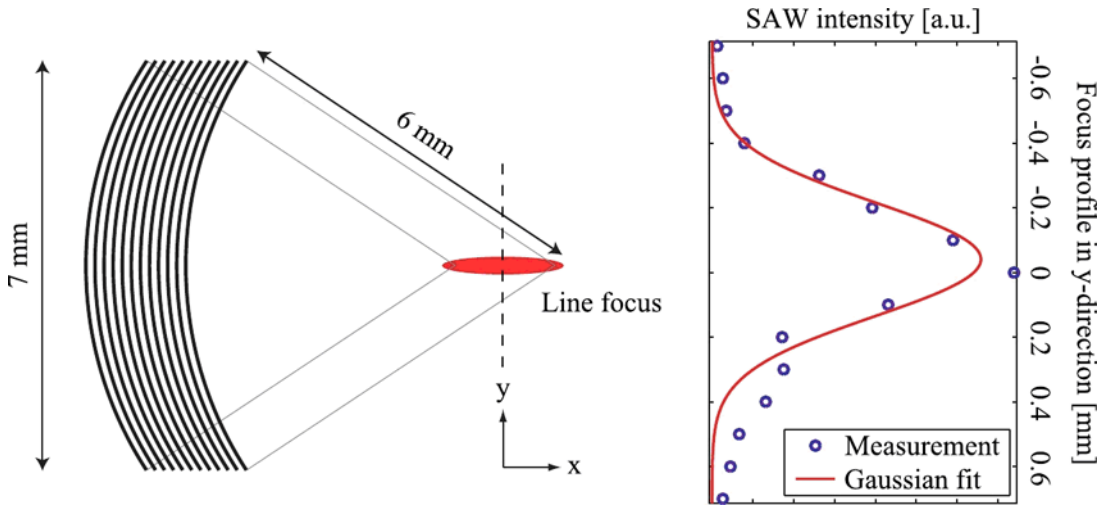

FIG. 3: (a) Schematic sketch of a circular grating. Since the radius is equal for all structures, the expected focus symmetry is a line focus. (b) Profile perpendicular to the propagation direction. The amplitude of the knife-edge signal, as shown in Fig.1(a), is used as a measure for the SAW-intensity across the focus.

IDTs, a thin Au film was evaporated in order to guarantee good tunnelling conditions. The IDT structures were driven by a HF (high-frequency) function generator at their resonance frequency, with pulse widths of few microseconds.

Fig.4 shows the result of the tunnelling response at different HF- and thus SAW amplitudes, where the maxima of the current response vary almost linearly with the HF amplitudes. This indicates that in the case of IDT-based measurements, not only the displacement of the surface itself, but also effects due to the electro-magnetic field, which travels along, gives rise to the STM signal.

In order to compare the data with our optical measurements, we created the same permanent laser interference gratings for SAW generation as denoted in section II for our STM measurements. As excitation laser, a single Nd:YAG pulse was used. Fig.5 shows typical STM results for different tunnelling set points at a SAW frequency of 14.6 MHz and an amplitude below 1 Å.

For low set points, only a very weak signal can be detected. With increasing currents, however, the STM signal I_{max} increases as well. The temporal delayed onset is due to the travelling distance between the excitation spot and the STM tip. If one calculates the relative current increase I_{rel} of a sinusoidally oscillating tunnelling gap with a fixed amplitude a and its exponential $I(z)$ characteristic, it follows thatI_{rel} is independent of the set point I_0 itself; see Eq. (1).

$$I_{rel} = \frac{\Delta I(a)}{I_0} = \frac{I_{\max}(a) - I_0}{I_0} = const \tag{1}$$

Exactly this behaviour is obtained by the analysis corresponding to Fig.5. Since a travelling SAW can be described as an oscillating tunnelling gap in the vicinity of the tip, the constant

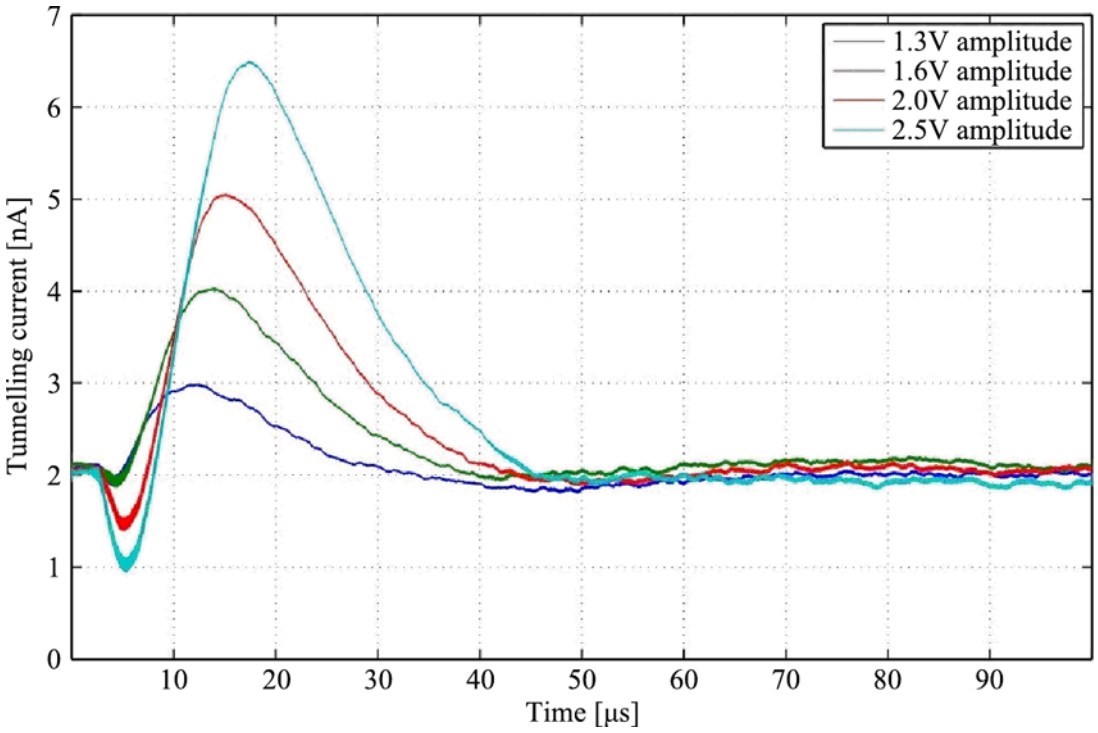

FIG. 4: With increasing HF-voltage, applied to the IDT structures on $LiNbO_3$, the tunnelling current signal increases linearly. This leads to the assumption that the current increase is not dominated by the expected exponential behaviour of the tunnelling gap.

value of $I_{rel} = 0.13 \pm 0.06$ shows that the rectification effect of the $I(z)$ curve is responsible for the signal. It holds for this frequency range and should also be valid in the GHz regime. Due to the rectification and the bandwidth restrictions of our I/U-converter, we only see something similar to the envelope of the SAW pulse. Therefore, we are mainly limited by the current noise in our system. Under ideal conditions, displacements as small as 10 pm could still be detected.

IV. CONCLUSIONS

We have shown that permanent laser interference patterns can easily be used to generate SAWs by illumination with additional ultra-short laser pulses. For a system like Au film on glass, the thermal expansion of the Au stripes is responsible for the launch of a SAW. Furthermore, the appropriate design of the generation patterns shows a route towards more complex SAW optics. In this paper, the effect of focussing has been demonstrated.

In order to overcome the optical limitation of spatial resolution, we have demonstrated the use of Scanning Tunnelling Microscopy. We generated SAWs by standard IDT structures on $LiNbO_3$ and showed the sensitivity of the tunnelling gap. Combination of both the

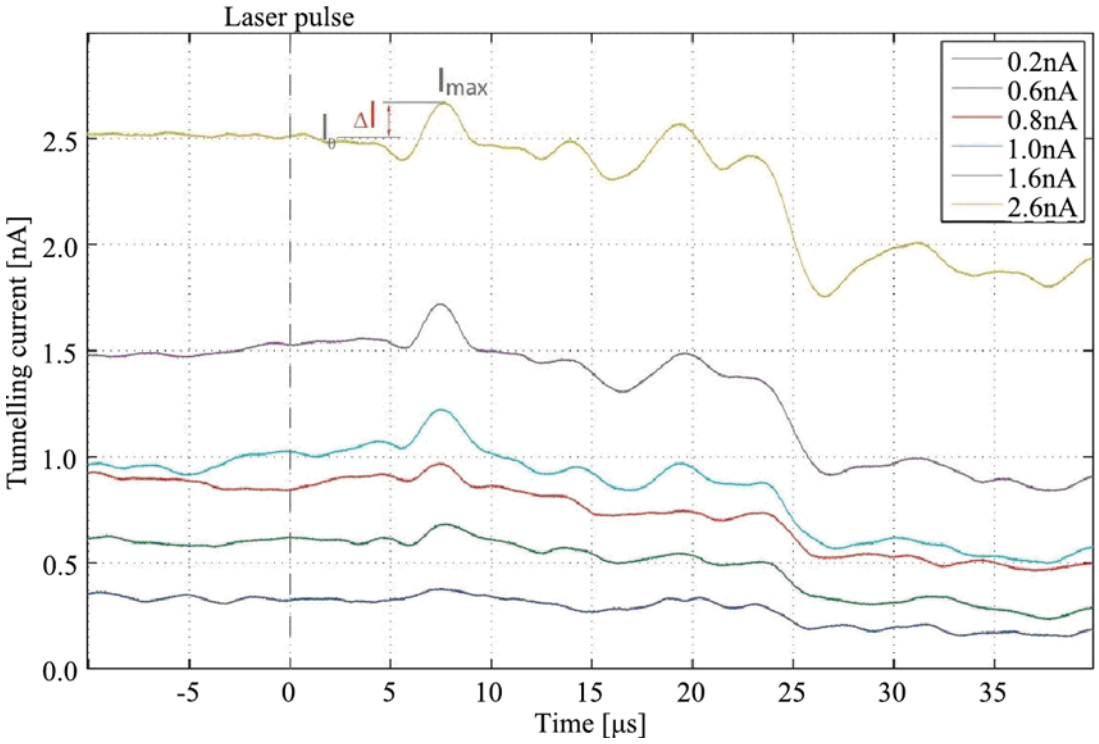

FIG. 5: Tunnelling current signals for 14.6-MHz SAWs excited by the laser illumination of a permanent grating on an Au film for increasing current set points. The signal onset is temporally shifted because of the distance between the excitation spot and the tunnelling tip.

optical excitation and the STM detection gave first promising results. Since the relative signal increase of the tunnelling current was independent of the set point, the signal has to be dominated by the effect of an oscillating tunnelling gap and thus is the result of the travelling SAW. The lowest detectable surface displacements could be estimated to be around 10 pm. Since SAW amplitudes in the GHz range can be as low as few pm, we reach the performance limit of this detection method.

Acknowledgments

We thank the group of Prof. Dr. Achim Wixforth for providing us with $LiNbO_3$ samples. The work presented in this paper was financially supported by the German Research Foundation DFG within the Collaborative Research Centre SFB 767 "Controlled Nanosystems."

References

* Electronic address: markus.schmotz@uni-konstanz.de

[1] R. Taubert *et. al.*, New J. Phys. **9**, 376 (2007)
[2] L. Rayleigh, Proc. London Math. Soc. **1**, 4 (1885)
[3] M. E. Siemens *et. al.*, Appl. Phys. Lett. **94**, 093103 (2009)
[4] S. Riedel *et. al.*, Appl. Phys. A, online first (2010)
[5] Yu. Kaganovskii *et. al.*, J. Appl. Phys. **100**, 044317 (2006)
[6] P. Leiderer *et. al.*, Appl. Phys. Lett. **85**, 5370 (2004)
[7] J. Boneberg *et. al.*, Appl. Phys. A **89**, 299 (2007)
[8] C. B. Scruby *et. al.*, Hilger, *Laser ultrasonics*, (1990)
[9] E. Lean, Prog. in Optics. **31**, 123 (1973)
[10] A. Yaoita *et. al.*, NDT & E International **38** (7), 554 (2005)
[11] P. Voigt *et. al.*, J. Appl. Phys. **92**, 7160 (2002)
[12] J. Jersch *et. al.*, Rev. Sci. Inst. **70**, 4579 (1999)
[13] T. Hesjedal *et. al.*, Appl. Phys. Lett. **69**, 354 (1996)